Letter

Thermodynamics of analogue black holes in a non-Hermitian tight-binding model

D. F. Munoz-Arboleda [1,*] M. Stålhammar [1,2] and C. Morais Smith [1]
[1]*Institute for Theoretical Physics, Utrecht University, 3584CC Utrecht, The Netherlands*
[2]*Department of Physics and Astronomy, Uppsala University, Uppsala, Sweden*

(Received 11 July 2025; accepted 22 January 2026; published 26 February 2026)

We present a non-Hermitian model with gain/loss and nonreciprocal next-nearest-neighbor hopping that emulates black-hole physics. The model describes a one-dimensional lattice with a smooth connection between regions with distinct hopping parameters. By mapping the system to an effective Schwarzschild metric in the Painlevé-Gullstrand coordinates, we find that the interface is an analogue to a black-hole event horizon. We obtain emission rates for particles and antiparticles, the Hawking temperature, the Bekenstein-Hawking entropy, and the mass of the analogue black hole as a function of the interface sharpness and the system parameters. An experimental realization of the theoretical model is proposed, thus opening the way to the detection of elusive black-hole features.

DOI: 10.1103/vdsx-r3dq

Introduction. For more than 50 years, one of the most intriguing findings in physics has been the black-hole (BH) process [1]. Hawking predicted that a quantum field placed in a curved spacetime background that describes a BH will emit thermal radiation [2]. One of the main difficulties in observing Hawking radiation is that, for the smallest astrophysical BH [3–5], the Hawking radiation is extremely weak, making it virtually impossible to observe [6–8]. One way to avoid this difficulty is by looking at primordial BHs (BHs created at the early stages of the universe). However, up to now, there is no record of this type of BH.

In 1981, Unruh introduced the concept of analogue gravity by showing that sound waves in a moving fluid could be described by an effective metric analogue to that of a BH, including an acoustic horizon and associated Hawking-like radiation [9]. This insight established the foundation for a broad interdisciplinary research program that demonstrated how controllable laboratory systems could emulate aspects of quantum field theory in curved spacetime. Subsequent theoretical developments extended this framework to a variety of media, identifying analogues of phenomena such as superradiance, cosmological particle production, and horizon backreaction in systems governed by effective metrics derived from fluid dynamics, optics, and condensed matter [8,10–12]. Experimental efforts confirmed these theoretical predictions, including the measurement of stimulated Hawking radiation in surface water waves under controlled flow conditions [10,12], as well as the generation of horizonlike effects using optical fibers and slow-light systems. In particular, the observation of spontaneous and entangled phonon emission in Bose-Einstein condensates provided strong evidence for quantum Hawking radiation in an analogue setting [13].

While these developments have been grounded in Hermitian physics, their extension to non-Hermitian (nH) systems has opened new avenues for understanding spacetime analogues and causal structures in dissipative or driven settings. Most traditional analogue BH implementations rely on real-valued wave equations and conserve probability, which restricts the range of phenomena that can be modeled. However, many realistic experimental platforms, including those involving gain/loss and amplification, operate in nH regimes. Recently, it was shown that nH Dirac-like systems with parity-time ($\mathcal{PT}$) symmetry can exhibit structures analogous to light cones in general relativity, with a well-defined effective line element that mimics causal flow near horizons [14,15]. This approach establishes a formal bridge between nH band structures and spacetime geometry, allowing phenomena such as horizon-induced tunneling or spectral flow to be recast in terms of complexified metrics. These results suggest that the inclusion of non-Hermiticity is not merely a perturbative feature but can play a central role in defining new classes of analogue gravitational systems.

The Painlevé-Gullstrand formulation of the Schwarzschild geometry is particularly well suited for analogue gravity models, as it allows for a clear description of radial flow and horizon structure without coordinate singularities [15–17]. In this coordinate system, the spacetime is foliated by spatial hypersurfaces that are flat but threaded by a velocity field representing the infall of a freely falling observer. This form of the metric bears a striking resemblance to the energy dispersion of nH lattice models, where the nonreciprocal hopping induces a directional energy flow and an effective group velocity that can be interpreted as a lattice analogue of gravitational infall. These coordinates are particularly important for describing Hawking and Unruh radiation, as they allow for a regular, observer-dependent formulation of horizon-crossing processes.

The Parikh-Wilczek approach provides an alternative perspective on Hawking radiation by modeling it as a quantum

*Contact author: d.f.munozarboleda@uu.nl

Published by the American Physical Society under the terms of the Creative Commons Attribution 4.0 International license. Further distribution of this work must maintain attribution to the author(s) and the published article's title, journal citation, and DOI. Funded by Bibsam.

tunneling process across the BH horizon, rather than as a phenomenon strictly related to global spacetime features [18]. In this semiclassical formulation, particles escape from the horizon through classically forbidden regions, and the resulting emission spectrum is nearly thermal, with corrections due to energy conservation and backreaction. This framework refines the original derivation by accounting for the self-interaction of the tunneling particle, and has become central in discussions of BH thermodynamics and quantum corrections to evaporation. In analogue gravity systems, this formalism offers a powerful tool to interpret emission processes as effective tunneling events, especially in contexts where the underlying dispersion relations are modified or complexified, as occurs in dispersive media or nH platforms.

In this Letter, we explore these connections by studying a nH tight-binding (TB) model that includes on-site gain/loss, as well as nonreciprocal next-nearest-neighbor (NNN) hopping. We show that this model exhibits a regime in which the NNN hopping across a spatial interface emulates the behavior of frequency modes near a BH horizon in Painlevé-Gullstrand coordinates. By analyzing the complex-valued dispersion relation near the interface, we demonstrate the emergence of an effective tunneling process, with an emission rate that is similar to that derived by Parikh-Wilczek [18]. This allows us to define a Hawking-like temperature and an associated Bekenstein-Hawking entropy from the lattice spectrum, revealing how thermodynamic features of BH evaporation can emerge from nH band structures.

This correspondence opens another route to exploring gravitational phenomena in controlled, tabletop settings using engineered nH materials. While analogue gravity models have been constructed in various fluid systems, Bose-Einstein condensates, and optical media [19,20], our approach highlights the potential of nH-TB lattices to capture not only kinematic aspects of BH analogues but also *thermodynamical* features. In particular, the incorporation of gain/loss enables a direct encoding of dissipative effects and information flow, which are essential to any quantum theory of gravity.

From a condensed-matter perspective, our findings illustrate how nH Hamiltonians can simulate relativistic geometries and thermodynamical processes beyond equilibrium. The emergent geometry in our model is not imposed externally but arises from the interplay of microscopic lattice parameters, suggesting different ways to engineer artificial spacetimes with tunable properties. This may pave the way for future investigations into analogue cosmology, topological gravity, and the holographic duality in nH settings.

nH-TB model. Non-Hermitian extensions of one-dimensional (1D) chains have garnered significant attention, particularly under $\mathcal{PT}$-symmetric conditions [21], where balanced gain and loss potentials lead to novel topological phenomena [22–24]. Here, we consider a $\mathcal{PT}$-symmetric nH-TB Hamiltonian H with N unit cells and two sublattices, A (cyan) and B (magenta) (see Fig. 1),

$$H = \sum_{j=1}^{N} [\tau(b_j^\dagger a_j + a_{j+1}^\dagger b_j + \text{H.c.}) + i\gamma(a_j^\dagger a_j - b_j^\dagger b_j) - \frac{\kappa}{2}(a_{j+1}^\dagger a_j - a_j^\dagger a_{j+1} + b_j^\dagger b_{j+1} - b_{j+1}^\dagger b_j)], \quad (1)$$

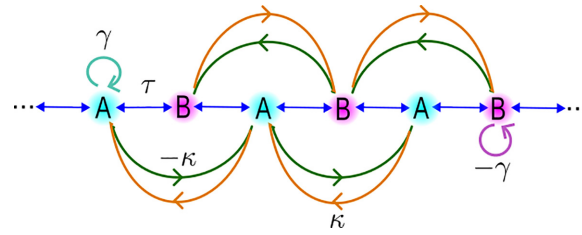


FIG. 1. Sketch of the nH-TB model. The blue lines describe the hopping parameter τ, the cyan (magenta) lines represent the gain (loss) potential γ $(-\gamma)$, and the green (orange) lines describe the nonreciprocal NNN hopping $-\kappa$ (κ).

that incorporates a hopping parameter τ, with $a_j^\dagger$ and $b_j^\dagger$ (a_j and b_j) the creation (annihilation) operators on sites A and B of the j_{th} unit cell, respectively, a balanced gain/loss $[\gamma/(-\gamma)]$ in the A and B sublattice, and a nonreciprocal NNN hopping parameter κ. Although there is no difference between the intracell and intercell hopping, it is possible to differentiate the sublattices A and B through the gain and loss potentials and the nonreciprocal NNN hopping. The lattice constant is put to unity. Using periodic boundary conditions (PBCs), we derive the Bloch Hamiltonian and expand $\sin(k)$ and $\cos(k)$ around π [25] to linear order

$$h(\tilde{k}) = \begin{pmatrix} i(\gamma + \kappa\tilde{k}) & +i\tau\tilde{k} \\ -i\tau\tilde{k} & -i(\gamma + \kappa\tilde{k}) \end{pmatrix}, \quad (2)$$

where $\tilde{k} = (k - \pi)$. Here, $h(\tilde{k})$ is $\mathcal{PT}$ symmetric $[h(\tilde{k}) = \sigma^x h^*(\tilde{k})\sigma^x]$ [26]. The eigenvalues are

$$\epsilon_\pm(\tilde{k}) = \pm\sqrt{\tau^2\tilde{k}^2 - (\gamma + \kappa\tilde{k})^2}, \quad (3)$$

and the system hosts exceptional points when $\gamma = -\kappa\tilde{k} \pm |\tau\tilde{k}|$, which form a cone with a tilting profile controlled by κ (see Fig. 2). A similar tilting profile can be found in the surroundings of a Schwarzschild BH event horizon in Painlevé-Gullstrand coordinates by tuning the free-falling velocity [16,27]. Hence, a relation between nH $\mathcal{PT}$-symmetric models and BHs becomes evident [15]. For $\kappa = 0$, we see a cone of exceptional points, which is tilted by the parameter κ. If $|\kappa| > 1$, the cone is overtilted (similar to a Lifshitz transition in Weyl materials) [28,29].

Analogue spacetime. To relate the exceptional cone (see Fig. 2, red lines) with the light cone of a Schwarzschild BH, we follow the procedure outlined in Ref. [15]. Noticing that γ takes the form of the eigenvalues of a Dirac operator, we promote it to an operator,

$$\hat{\gamma} = -\kappa\tilde{k}\sigma^0 + |\tau\tilde{k}|\sigma^x \to \hat{\gamma} = e^\mu{}_\alpha \tilde{k}_\mu \sigma^\alpha, \quad (4)$$

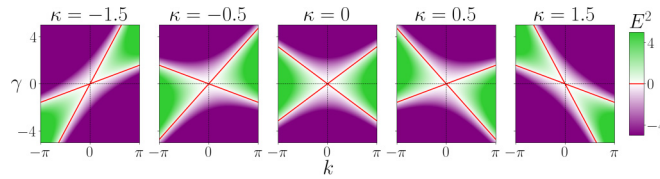


FIG. 2. Behavior of the energy square (see color code) as a function of γ and k for different values of κ. For simplicity, $\tau = 1$. Red lines indicate the exceptional points.

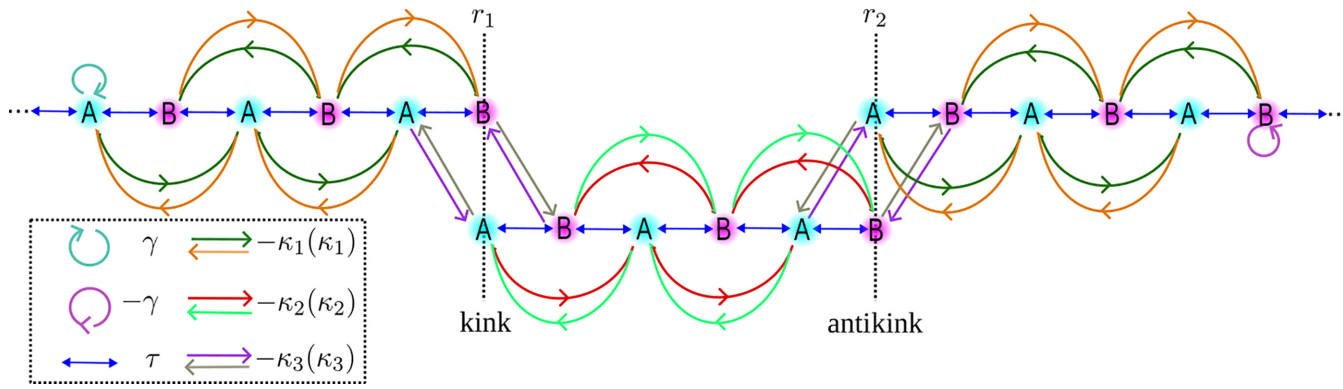


FIG. 3. Sketch of the two coupled gain/loss nH-TB chains with nonreciprocal NNN hopping. The blue line represents the nearest-neighbor hopping parameter τ. The green (orange) line represents the NNN hopping parameter κ_1 (κ_2) for the first chain (second chain). The purple (gray) line represents the NNN hopping parameter (κ_3) between A (B) sites through the interface between the first and second chain, mimicking the horizon of the BH.

where $e^{\mu}{}_{\alpha}$ are vielbeins or tetrad fields [30–33], $\mu, \alpha \in \{0, 1\}$, $\sigma^0 = \mathbf{1}$, and σ^1 is a Pauli matrix. The vielbeins give rise to a metric of the form $g^{\mu\nu} = e^{\mu}{}_{\alpha} e^{\nu}{}_{\beta} \eta^{\alpha\beta}$ where $\eta^{\alpha\beta} = \mathrm{diag}(-1, 1)$. Thus, a line element of the spacetime is obtained as $ds^2 = g_{\mu\nu} dx^{\mu} dx^{\nu}$. For the nH-TB model defined above, the vielbeins are $e^0_0 = 1$, $e^1_1 = \tau$, and $e^1_0 = -\kappa$. Without losing generality, we fix $\tau = 1$. Then, the line element can be written as

$$ds^2 = -(1 - \kappa^2)(dt)^2 + 2\kappa dt dx + (dx)^2, \tag{5}$$

which is similar to the Schwarzschild metric in the Painlevé-Gullstrand coordinates

$$ds^2 = -\left(1 - \frac{2M_o}{r}\right)(dt_r)^2 + 2\sqrt{\frac{2M_o}{r}} dt_r dr, \tag{6}$$

with M_o denoting the mass at the event horizon for a freely falling observer [16–18,34,35]. In Eq. (5), if κ is positive (negative) we obtain the analogue of a black (white) hole.

Analogue event horizons through coupled chains. Since the nH-TB model described above can be related to the metric of a Schwarzschild BH in the Painlevé-Gullstrand coordinates, we now construct a model that allows us to mimic the corresponding event horizon. To do so, we couple two nH-TB chains with on-site gain/loss γ, a hopping parameter $\tau = 1$, and NNN hopping κ_1 and κ_2, respectively. The two chains are connected by smooth interfaces with a kink (antikink) at position r_1 (r_2), and the NNN hopping across the interfaces is $\pm\kappa_3$.

The setup is illustrated in Fig. 3, where we assume PBC. The first chain represents the inside of the BH, and the second chain represents the outside. The kink (antikink) represents the transition point in real space from the first to the second (second to the first) chain, which is analogous to an event horizon. The Bloch Hamiltonian describing this system reads

$$h(k) = \begin{pmatrix} i[\gamma - f(r)\sin(k)] & 1 + e^{-ik} \\ 1 + e^{ik} & -i[\gamma - f(r)\sin(k)] \end{pmatrix}, \tag{7}$$

where $f(r)$ is assumed to have the form

$$f(r) = \kappa_1 + \frac{\kappa_1 - \kappa_2}{2}\left[\tanh\frac{(r_1 - r)}{l} + \tanh\frac{(r - r_2)}{l}\right], \tag{8}$$

and thus readily include the NNN hopping of each individual chain: $f(r) \sim \kappa_1$ for $r < r_1$, $r > r_2$, and $f(r) \sim \kappa_2$ for $r_1 < r < r_2$, and $f(r_1) = f(r_2) = (\kappa_1 + \kappa_2)/2 = \kappa_3$. In Eq. (8), l is the width of the domain wall. Performing the same expansion as in Eq. (2), we find $h(\tilde{k}) = -\tilde{k}\sigma^y + i[\gamma + f(r)\tilde{k}]\sigma^z$. The corresponding cone of exceptional points is described by $\gamma = -f(r)\tilde{k} \pm |\tilde{k}|$.

However, the explicit spatial dependence of the function $f(r)$ makes the commutation relation $[\tilde{k}, h(\tilde{k})]$ nonvanishing, since

$$[\tilde{k}, h(\tilde{k})] = \tilde{k}\frac{\partial f(r)}{\partial r}. \tag{9}$$

We have neglected these contributions when solving the eigenvalue equation. Close to the analogue horizon $r \to r_1$ in a sufficiently large chain, i.e., $r_1 \ll r_2$, this amounts to assuming

$$\left|\frac{\kappa_2 - \kappa_1}{2l}\tilde{k}\right| \ll |\gamma|, \quad \left|\frac{\kappa_2 - \kappa_1}{2l}\right| \ll |\tau|, \tag{10}$$

which define the parameter ranges in which the lattice model mimics the interior and exterior of a BH, as well as the corresponding event horizon.

Following the same procedure as in the previous section, the metric for this particular model is

$$ds^2 = -[1 - f^2(r)]dt^2 + 2f(r)drdt + dr^2. \tag{11}$$

We now want to find where Eq. (11) describes a Schwarzschild-like BH. This can be done by expanding Eqs. (6) and (11) to linear order in $(r - 2M_o)$ and $(r - r_1)$, respectively, and equating order by order to ensure identical behaviors at and close to the horizon,

$$\frac{\kappa_1 + \kappa_2}{2} - \frac{\kappa_1 - \kappa_2}{2l}(r - r_1) = 1 - \frac{1}{4M_o}(r - 2M_o). \tag{12}$$

Equation (12) defines the horizon in terms of the model parameters, namely

$$\kappa_3 = \frac{\kappa_1 + \kappa_2}{2} = 1, \quad r_1 = 2M_o, \quad \text{and} \quad \frac{\kappa_1 - \kappa_2}{2l} = \frac{1}{2r_1}, \tag{13}$$

which bounds the NNN hopping parameters to $\kappa_1 > 1$, $\kappa_2 < 1$, and $\kappa_3 = 1$.

Semiclassical limit and emission rate. Having established the relation between our nH-TB model and the Schwarzschild BH, we now turn to the corresponding BH evaporation. This is done by studying the tunneling process close to the horizon using the Parikh-Wilczek method [18], which takes two processes contributing to the spontaneous emission of massless particles into account. One is obtained from a particle tunneling outwards the interior of the BH, and the other one comes from an antiparticle tunneling into the BH. In Fig. 2, we depict with red lines the region in momentum space that corresponds to the exceptional cone, which is analogous to the lightlike shell of energy seen by a radially falling observer. The momentum of a quantum massless particle or antiparticle follows the radial falling trajectories (radial null geodesics) [36,37], hence $\dot{r}^{\pm} \to p_r^{\pm}$. In our lattice model, $\tilde{k}^{\pm}$ is the analogue of the conjugate momentum $p_r^{\pm}$. On the exceptional cone, we obtain

$$\tilde{k}_r^{\pm} = \frac{\gamma f(r)}{1-f^2(r)} \pm \sqrt{\frac{\gamma^2}{[1-f^2(r)]^2}}. \tag{14}$$

Now, we need to identify which solution is related to the analogue of the particle and the antiparticle channel. Usually, the method for determining the particle and antiparticle channels comes from the behavior of $\tilde{k}^{\pm}(r)$ when approaching the asymptotic infinity. In our analogue model the asymptotic infinity lies in $r_1 < r < r_2$; it is bound because of the PBCs. For a sufficeintly large second chain, there exists an r_∞ such that $r_1 \ll r_\infty \ll r_2$, and consequently $f(r_\infty) \sim \kappa_2$. Then, we get

$$\tilde{k}_r^{\pm}(r_\infty) = \frac{\gamma\kappa_2}{1-\kappa_2^2} \pm \left\{\frac{\gamma^2}{\left[1-\kappa_2^2\right]^2}\right\}^{1/2}. \tag{15}$$

From the conditions given in Eq. (13), we know that $0 < \kappa_2 < 1$ and obtain $\tilde{k}_r^{+} \geqslant 0$ and $\tilde{k}_r^{-} \leqslant 0$. These equations describe the analogue momentum of a particle ($\tilde{k}_r^{+}$) and an antiparticle ($\tilde{k}_r^{-}$) for any real value of γ. The classically forbidden process is obtained by computing the imaginary part of the action $\mathrm{Im}(S^{\pm}) = \mathrm{Im}(\int dr \tilde{k}_r^{\pm}) = I^{\pm}$ [15,18]. These solutions correspond to the particle (+) and antiparticle (−) channels involved in the tunneling process; the particle channel describes a positive-frequency ($\omega > 0$) particle tunneling out from the BH, while the antiparticle channel describes a negative-frequency ($\omega' < 0$) antiparticle tunneling into the BH. As explained above, this implies that (anti)particles radiate out from (into) the BH interior, causing the BH mass to decrease from M_o to $M_o - \omega$ ($M_o + \omega'$), which in turn leads to a shrinking of the horizon. Taking the change in mass into account, the integration limits around the horizon are set as $r_{\mathrm{in}} = r_1$ and $r_{\mathrm{out}} = r_1 - 2\omega$ ($r_{\mathrm{out}} = r_1 + 2\omega'$), where $r_1 = 2M_o$ is obtained from Eq. (12). Inserting $\tilde{k}_r^{\pm}$ into $\mathrm{Im}(S^{\pm})$, we obtain $I^{\pm}$. By solving the integral for the particle and antiparticle channel, and recalling that both channels contribute to the probability of the tunneling process [18], we obtain the semiclassical emission rate [15,18]

$$\Gamma \propto (\mathcal{A}^{+} + \mathcal{A}^{-})^2 = e^{-8\pi M_o|\gamma|} = e^{\Delta S_{\text{B-H}}}, \tag{16}$$

where $\mathcal{A}^{\pm} = \exp(-I^{\pm})$. Detailed calculations are provided in a Supplemental Material [38]. The above equation shows the relation between the exponential part of the semiclassical emission rate and the change in the Bekenstein-Hawking entropy ($\Delta S_{\text{B-H}}$) [2,18,39–42], which leads to

$$\Delta S_{\text{B-H}} = -8\pi M_o|\gamma| = -4\pi|\gamma|\frac{l}{\kappa_1-\kappa_2}. \tag{17}$$

Thermodynamics of the analogue BH. To complement the calculation of $\Delta S_{\text{B-H}}$, we compute the difference in the thermal entropy ΔS from thermodynamic principles $dM = T_{\text{H}} dS$, where $T_{\text{H}} = 1/8\pi M$ is the Hawking temperature of a Schwarzschild BH. Comparing Eqs. (6) and (11) term by term, we can obtain a relation between the mass M of the BH and the function $f(r)$ that describes the behavior of the NNN hopping through the chains. Notice that we are interested in a variable mass M and not only in the mass at the event horizon M_o. The thermal entropy is written as

$$\Delta S = \int_{M_o}^{M_o-\omega} 8\pi M dM = -\frac{3\pi}{2}\left(\frac{l}{\kappa_1-\kappa_2}\omega + \omega^2\right). \tag{18}$$

Equating $\Delta S_{\text{B-H}} = \Delta S$, we get $-8\pi M|\gamma| = -3\pi(2M\omega + \omega^2)/2$. In terms of the lattice parameters, the frequency reads

$$\omega^{\pm} = -\frac{l}{2(\kappa_1-\kappa_2)} \pm \sqrt{\frac{l^2}{4(\kappa_1-\kappa_2)^2} + \frac{8l|\gamma|}{3(\kappa_1-\kappa_2)}}. \tag{19}$$

Recalling Eq. (10), $(\kappa_1 - \kappa_2)/2l \ll 1$, the leading-order contribution to the frequency becomes $\omega^{+} = 8|\gamma|/3$. This remarkably simple relation indicates that the frequency of the emitted particles responsible for the BH evaporation, and hence the semiclassical emission rate, is controlled exclusively by the gain/loss parameter. Practically, this means that the nature of different BH evaporation processes can be scanned through in our model by simply tuning the on-site potential.

Discussion. We introduced a nH-TB model with $\mathcal{PT}$-symmetric gain/loss and nonreciprocal NNN hopping, which gives rise to exceptional cones with tunable tilt. By expanding the Bloch Hamiltonian near the Brillouin zone edge, we revealed Dirac-like operators that mimic light cones in curved spacetime. Mapping the cone tilt to Painlevé-Gullstrand coordinates, we identified a correspondence with Schwarzschild black holes. This analogy enables us to design a tabletop setup with two smoothly connected chains, emulating a black-hole horizon with interior, exterior, and interface regions.

To examine tunneling across the analogue horizon, we employed a semiclassical approach inspired by the Parikh-Wilczek method [18], deriving an emission rate governed by the change in B-H entropy. Additionally, by analyzing the thermodynamic response of the system, we obtained a compact expression linking the emission frequency to the on-site gain/loss parameter, $\omega^{+} = 8|\gamma|/3$. The quadratic contribution in our entropy balance, $-8\pi M|\gamma| = -3\pi(2M\omega + \omega^2)/2$, is a consequence of the energy conservation in the tunneling process, in direct analogy with the Parikh-Wilczek correction to strict thermality.

Our results provide a concrete example of how nH topological models can simulate aspects of BH physics, including horizon dynamics and Hawking-like radiation. In a tabletop realization, the analogue "particle/antiparticle" channels correspond to the correlated creation of two excitations in distinct

mode sectors generated by horizon-induced mode conversion (e.g., opposite group velocities or opposite branches of the effective dispersion), rather than to literal matter-antimatter emission. Operationally, these channels are therefore most naturally identified through correlations between signals measured on the exterior and interior sides of the interface or between two frequency bands, accessible via transmission and reflection spectra, time-resolved wave-packet scattering, and two-point correlation measurements. Moreover, since the horizon location is set by $r_1 = 2M_o$ and the emitted energy lowers the effective mass to $M_o - \omega$ with $\omega = 8|\gamma|/3$, the corresponding time-dependent motion of the interface can be emulated experimentally by tracking the evolution of a Gaussian wave function or a two-point spatial correlation function across the horizon.

The implementation of our model in an experimental setup is of great interest because it can yield insight into the nature of BH evaporation, the emission rate due to tunneling processes near the event horizon, and the thermodynamics of such systems. Platforms capable of realizing gain/loss potentials and nonreciprocal contributions simultaneously include photonic crystals [43], topoelectric circuits [44,45], and robotic metamaterials [46], to cite just a few. By measuring the local density of states in the model described here, a relation between the probability of the emission rate of particles and antiparticles, the Hawking temperature, and the thermal entropy can be obtained.

Acknowledgments. The authors thank R. Arouca for the valuable discussions. D.F.M.-A. acknowledges funding from the Colombian Ministry of Science (Minciencias) and CMS acknowledges funding from QuMat, a program of the Netherlands organization for Scientific Research (NWO) that is funded by the Dutch Ministry of Education, Culture and Science. M.S. is supported by the Swedish Research Council (VR) under Grant No. 2024.00272.

Data availability. The data that support the findings of this article are not publicly available. The data are available from the authors upon reasonable request.

[1] S. W. Hawking, Black hole explosions? Nature (London) **248**, 30 (1974).
[2] S. W. Hawking, Particle creation by black holes, Commun. Math. Phys. **43**, 199 (1975).
[3] S. Chandrasekhar, The maximum mass of ideal white dwarfs, Astrophys. J. **74**, 81 (1931).
[4] J. R. Oppenheimer and H. Snyder, On continued gravitational contraction, Phys. Rev. **56**, 455 (1939).
[5] R. Abbott, T. D. Abbott, S. Abraham, F. Acernese, K. Ackley, C. Adams, R. X. Adhikari, V. B. Adya, C. Affeldt, M. Agathos, *et al.*, GW190814: Gravitational waves from the coalescence of a 23 solar mass black hole with a 2.6 solar mass compact object, Astrophys. J. Lett. **896**, L44 (2020).
[6] B. J. Carr and S. W. Hawking, Black holes in the early universe, Mon. Not. R. Astron. Soc. **168**, 399 (1974).
[7] B. J. Carr, S. Clesse, J. García-Bellido, M. R. S. Hawkins, and F. Kühnel, Observational evidence for primordial black holes: A positivist perspective, Phys. Rep. **1054**, 1 (2024).
[8] C. Barceló, S. Liberati, and M. Visser, Analogue gravity, Living Rev. Relativ. **14**, 3 (2011).
[9] W. G. Unruh, Experimental black-hole evaporation? Phys. Rev. Lett. **46**, 1351 (1981).
[10] S. Weinfurtner, E. W. Tedford, M. C. J. Penrice, W. G. Unruh, and G. A. Lawrence, Measurement of stimulated hawking emission in an analogue system, Phys. Rev. Lett. **106**, 021302 (2011).
[11] V. Subramanyan, S. S. Hegde, S. Vishveshwara, and B. Bradlyn, Physics of the inverted harmonic oscillator: From the lowest Landau level to event horizons, Ann. Phys. **435**, 168470 (2021).
[12] S. Patrick, H. Goodhew, C. Gooding, and S. Weinfurtner, Backreaction in an analogue black hole experiment, Phys. Rev. Lett. **126**, 041105 (2021).
[13] J. Steinhauer, Observation of quantum Hawking radiation and its entanglement in an analogue black hole, Nat. Phys. **12**, 959 (2016).
[14] S. Longhi, Non-Hermitian Dirac cones, Phys. Rev. Lett. **124**, 066602 (2020).
[15] M. Stålhammar, J. Larana-Aragon, L. Rødland, and F. K. Kunst, $\mathcal{PT}$ symmetry-protected exceptional cones and analogue Hawking radiation, New J. Phys. **25**, 043012 (2023).
[16] P. Painlevé, La mécanique classique et la théorie de la relativité, L'Astronomie **36**, 6 (1922).
[17] G. E. Volovik, Simulation of a Panlevé-Gullstrand black hole in a thin ^{3}He-A film, J. Exp. Theor. Phys. Lett. **69**, 705 (1999).
[18] M. K. Parikh and F. Wilczek, Hawking radiation as tunneling, Phys. Rev. Lett. **85**, 5042 (2000).
[19] Y. Rosenberg, Optical analogues of black-hole horizons, Philos. Trans. R. Soc. A **378**, 20190232 (2020).
[20] J. Drori, Y. Rosenberg, D. Bermudez, Y. Silberberg, and U. Leonhardt, Observation of stimulated hawking radiation in an optical analogue, Phys. Rev. Lett. **122**, 010404 (2019).
[21] C. M. Bender and S. Boettcher, Real spectra in non-Hermitian Hamiltonians having $\mathcal{PT}$ symmetry, Phys. Rev. Lett. **80**, 5243 (1998).
[22] E. J. Bergholtz, J. C. Budich, and F. K. Kunst, Exceptional topology of non-Hermitian systems, Rev. Mod. Phys. **93**, 015005 (2021).
[23] K. Yang, Z. Li, J. L. K. König, L. Rødland, M. Stålhammar, and E. J. Bergholtz, Homotopy, symmetry, and non-Hermitian band topology, Rep. Prog. Phys. **87**, 078002 (2024).
[24] E. Slootman, W. Cherifi, L. Eek, R. Arouca, E. J. Bergholtz, M. Bourennane, and C. M. Smith, Breaking and resurgence of symmetry in the non-Hermitian Su-Schrieffer-Heeger model in photonic waveguides, Phys. Rev. Res. **6**, 023140 (2024).
[25] If we expand around zero, we would obtain an extra term 2τ and the calculations lead a Dirac-like operator that gives an exceptional cone with a shift in the momentum and does not change the physics of the system.
[26] A. Montag and F. K. Kunst, Essential implications of similarities in non-Hermitian systems, J. Math. Phys. **65**, 122101 (2024).
[27] A. J. S. Hamilton and J. P. Lisle, The river model of black holes, Am. J. Phys. **76**, 519 (2008).

[28] G. E. Volovik, Topological Lifshitz transitions, Low Temp. Phys. **43**, 47 (2017).
[29] W. Wu, Z. Shi, Y. Du, Y. Wang, F. Qin, X. Meng, B. Liu, Y. Ma, Z. Yan, M. Ozerov, C. Zhang, H.-Z. Lu, J. Chu, and X. Yuan, Topological Lifshitz transition and one-dimensional Weyl mode in $HfTe_5$, Nat. Mater. **22**, 84 (2023).
[30] S. M. Carroll, *Spacetime and Geometry: An Introduction to General Relativity* (Cambridge University Press, Cambridge, UK, 2019).
[31] T. Ortín, *Gravity and Strings*, Cambridge Monographs on Mathematical Physics (Cambridge University Press, Cambridge, UK, 2004).
[32] G. Volovik and M. Zubkov, Emergent Weyl spinors in multifermion systems, Nucl. Phys. B **881**, 514 (2014).
[33] P. Hořava, Stability of Fermi surfaces and K theory, Phys. Rev. Lett. **95**, 016405 (2005).
[34] G. Lemaitre, The expanding universe, Ann. Soc. Sci. Bruxelles, Ser. A **53**, 51 (1997).
[35] L. Vanzo, G. Acquaviva, and R. D. Criscienzo, Tunnelling methods and Hawking's radiation: Achievements and prospects, Class. Quantum Grav. **28**, 183001 (2011).
[36] N. D. Birrell and P. C. W. Davies, *Quantum Fields in Curved Space* (Cambridge University Press, Cambridge, UK, 1982).
[37] R. M. Wald, *Quantum Field Theory in Curved Spacetime and Black Hole Thermodynamics* (University of Chicago Press, Chicago, 1994).
[38] See Supplemental Material at http://link.aps.org/supplemental/10.1103/vdsx-r3dq for a detailed calculation of the imaginary part of the action.
[39] E. Keski-Vakkuri and P. Kraus, Microcanonical D-branes and back reaction, Nucl. Phys. B **491**, 249 (1997).
[40] S. Massar and R. Parentani, How the change in horizon area drives black hole evaporation, Nucl. Phys. B **575**, 333 (2000).
[41] J. D. Bekenstein, Black holes and the second law, Lett. Nuovo Cimento **4**, 737 (1972).
[42] J. D. Bekenstein, Black holes and entropy, Phys. Rev. D **7**, 2333 (1973).
[43] M. Reisenbauer, H. Rudolph, L. Egyed, K. Hornberger, A. V. Zasedatelev, M. Abuzarli, B. A. Stickler, and U. Delić, Non-Hermitian dynamics and non-reciprocity of optically coupled nanoparticles, Nat. Phys. **20**, 1629 (2024).
[44] C. H. Lee, S. Imhof, C. Berger, F. Bayer, J. Brehm, L. W. Molenkamp, T. Kiessling, and R. Thomale, Topolectrical Circuits, Commun. Phys. **1**, 39 (2018).
[45] D. Halder, R. Thomale, and S. Basu, Circuit realization of a two-orbital non-Hermitian tight-binding chain, Phys. Rev. B **109**, 115407 (2024).
[46] M. Brandenbourger, X. Locsin, E. Lerner, and C. Coulais, Non-reciprocal robotic metamaterials, Nat. Commun. **10**, 4608 (2019).